ELSEVIER

Carbohydrate Research 267 (1995) 161–166

CARBOHYDRATE RESEARCH

Note

Imaging xanthan gum by atomic force microscopy

Andrew R. Kirby, A. Patrick Gunning, Victor J. Morris *

Institute of Food Research, Norwich Research Park, Colney, Norwich NR4 7UA, United Kingdom

Received 29 June 1994; accepted 2 September 1994

Keywords: Atomic force microscopy; Scanning tunnelling microscopy; Xanthan; Polysaccharide; Biomolecule

Scanning probe microscopes (SPM) have revolutionised microscopy. Both the scanning tunnelling microscope (STM) and the atomic force microscope (AFM) have been used to image biopolymers [1–3]. Scanning probe microscopes offer the prospect of superior resolution to that obtained using present electron microscopy (EM) methods. Images can be obtained under near 'native' conditions, thus avoiding the harsh and damaging preparative and imaging procedures used in EM studies. Most of the early SPM studies of biological macromolecules were made using STM. Despite early success, biological STM has now encountered a number of problems which have dampened the early enthusiasm for the technique: the imaging mechanism for large macromolecules is unknown [1–3], and certain substrate features (particularly on graphite) can mimic biopolymers giving rise to imaging artifacts [4,5]. In addition, imaging is generally not reproducible, probably because of tip–molecule interactions which sweep the molecules outside the field of view [6–9]. Many of these difficulties are emphasised in the small number of papers reporting STM studies of polysaccharides [10–19]. The quality of the images previously presented has been disappointing, and most of the studies have not been reproduced by other workers.

Three groups have reported STM studies of the bacterial polysaccharide xanthan gum [15–17]. Miles and co-workers [15] presented a single STM image of xanthan molecules deposited from aqueous solution and then air-dried onto a graphite substrate. The image contains features consistent with the molecular structure of xanthan but other researchers have been unable to reproduce such data using the same preparative and imaging conditions [16,17]. Gunning and co-workers [16] obtained STM images of xanthan after depositing the molecules from aligned, concentrated 'liquid crystalline' preparations which were then air-dried onto graphite. The images revealed aggregates containing bundles of aligned xanthan molecules. The aggregation made resolution of individual molecules difficult.

* Corresponding author.

SSDI 0008-6215(94)00294-0

Wilkins and co-workers [17] reported comparative EM and STM studies of xanthan. These authors resorted to the use of spray deposition followed by metal coating. Such treatment has produced the most reliable images of xanthan obtained by STM at the present time. Although these preparative methods remove the inherent difficulties with the use of STM, they also effectively throw away the advantages of the technique. The resolution achieved is the same as that found by EM methods. This is because the resolution is limited by the grain size of the coating (~ 5 nm) which in itself prohibits any information being obtained on molecular architecture. Clearly there is a need to develop methods for reliably imaging uncoated polysaccharides. Many of the difficulties encountered with STM are absent when using the newer technique of AFM: the imaging mechanism is better understood and, since the imaging force can be controlled, sweeping or damage of molecules can be minimised or avoided. However, AFM is not yet at the stage where it can be applied to image routinely every biomolecule at molecular resolution. This is principally because the role of the various forces present in any given system is not fully understood. At the present time there is only one preliminary AFM study of a carbohydrate and this describes measurements on xanthan deposited onto mica [20]. This note reports more detailed studies of xanthan deposited onto mica. AFM images have been obtained using a new method which permitted highly reproducible imaging. The results obtained in the present study are discussed in the light of previous STM and AFM data.

The xanthan sample used in this study was Keltrol (Kelco-AIL). The powdered material was dispersed in water, heated to 85°C for 1 h whilst stirring, and then cooled to room temperature. A 0.1% (w/v) sample was centrifuged at 150 000*g* for 3 h (room temperature) and then stored overnight at 1°C. The sample was warmed to room temperature and diluted to a concentration of $\sim 20\ \mu g\ mL^{-1}$. A 2-μL drop was deposited onto freshly cleaved mica and allowed to dry in air for 10 min. The sample was then imaged under 1-butanol (Sigma Chemicals). 1-Butanol was chosen for several reasons. Imaging biopolymers on mica in air with standard AFM tips is difficult because of the presence of a thin layer of water on top of the sample when it is in ambient conditions (i.e., RH > 30%). This water layer gives rise to a capillary force which rams the AFM tip onto the surface with a force that is typically many times greater than the maximum force which fragile biomolecules can tolerate without damage [21,22]. This effect can be avoided by imaging under water, thereby removing the meniscus at the tip–sample interface. Unfortunately with the water–mica system there is another effect which manifests itself as a large adhesive force between the AFM tip and the mica surface [23]. This effect which is not fully understood can be minimised by imaging under alcohol instead of water. Such alcohols as 1-butanol provide the additional benefit that they are precipitants for polysaccharides and thus might be expected to inhibit desorption from the mica surface. Also these solvents have proved very useful for reliable imaging of nucleic acids [24–28]. The atomic force microscope used was an ECS (East Coast Scientific, Cambridge, UK) apparatus. The head, electronics, and software were designed by Mark Welland, Martin Murrell, and Tim Wong (Department of Engineering, Cambridge University, UK) and are now marketed by ECS. The experimental sample was contained in a liquid cell and imaged using constant force conditions. Using the liquid cell it has been noticed that the absolute value of the force may drift during scanning (probably due to thermal effects). With the ECS instrument it is possible to monitor and correct for this drift between scans. The optimum imaging conditions used forces ~ 3–4 nN. The tips used were

Nanoprobe cantilevers (Digital Instruments), the short narrow variety, with a nominal force constant of 0.38 N m^{-1}.

Fig. 1 shows representative images obtained for xanthan samples. The images (Figs. 1a–d) show areas of low polymer coverage within which individual xanthan molecules can be seen. These images are similar to those obtained by STM and EM of spray-deposited, metal-coated xanthan preparations [17]. The molecular thickness is variable and appears greatest for molecules aligned perpendicular to the scan direction. Typical thicknesses are ca. 10 nm which is nearly an order of magnitude greater than that expected for xanthan in the helical structure [29]. This effect is probably due to probe broadening, as a result of the finite curvature of the probe. Similar effects have been observed with DNA, which is a helical biopolymer with a comparable thickness [24–28], where the smallest observed width using standard tips was ca. 9 nm. In the case of DNA the use of supertips has improved resolution by reducing probe broadening [28]. Ends of molecules can be observed in Fig. 1 and images show a polydisperse preparation with contour lengths varying from less than 100 nm to sizes of >1 μm. Xanthan in the helical form has a Kuhn statistical segment length of 200 nm [29] and the images shown in Figs. 1a–d are characteristic of such extended stiff coils. As can be seen in the 3D image (Fig. 1b) the bright spots in Fig. 1a indicate that one molecule has crossed over a second molecule (arrow A). This permits distinction between regions where the molecules cross (arrow A, Fig. 1a) and regions where they meet side-by-side (arrow B, Fig. 1a). Thus it is possible to identify regions where molecules form loops (arrow C, Fig. 1a) or bifurcate (arrow D, Fig. 1a). These loops or bifurcations have been noted in spray-deposited, metal-coated images where they have been attributed to unravelling of a xanthan double helix into individual strands [17]. Care needs to be exercised in such interpretation since, as will be shown later, xanthan does appear to supercoil.

Most images were obtained at constant force. Figs. 1a and c illustrate the effects of allowing the force to vary during scanning. In Fig. 1a the force has decreased during scanning. At the bottom of the picture the imaging force is ca. 3–4 nN. This then decreases to a value of <1 nN at the top of the picture. As can be seen the major effect is to reduce the image contrast for the xanthan molecules. Fig. 1c shows the effect of allowing the force to increase during scanning. At the top of the picture forces of the order of 8–10 nN are sufficiently large to cause some distortion and damage to the molecules. Optimum contrast without sample damage is obtained for forces in the range 3–4 nN (Fig. 1d). It should be noted that these values for the imaging force are nominal since the spring constant of the levers can vary from their quoted specification [30].

Despite xanthan being an extremely stiff extended macromolecule, Fig. 1d illustrates that the molecule can form intra- and inter-molecular supercoils (arrows A, Fig. 1d). Thus in regions where bifurcations are observed (arrows B, Fig. 1d) it is difficult to distinguish between unravelling of supercoiled molecules or separation of individual strands in a double helix. However, it is possible that the drying process could have some influence over the conformation of the molecules.

Pictures shown in Figs. 1a–d represent dilute regions within which individual molecules can be seen. The air-drying process tends to concentrate the molecules into aggregated regions on the mica substrate. The edge of such an aggregate is shown in Fig. 1e. As the centre of the aggregate is approached the networks become more intertwined. It is possible

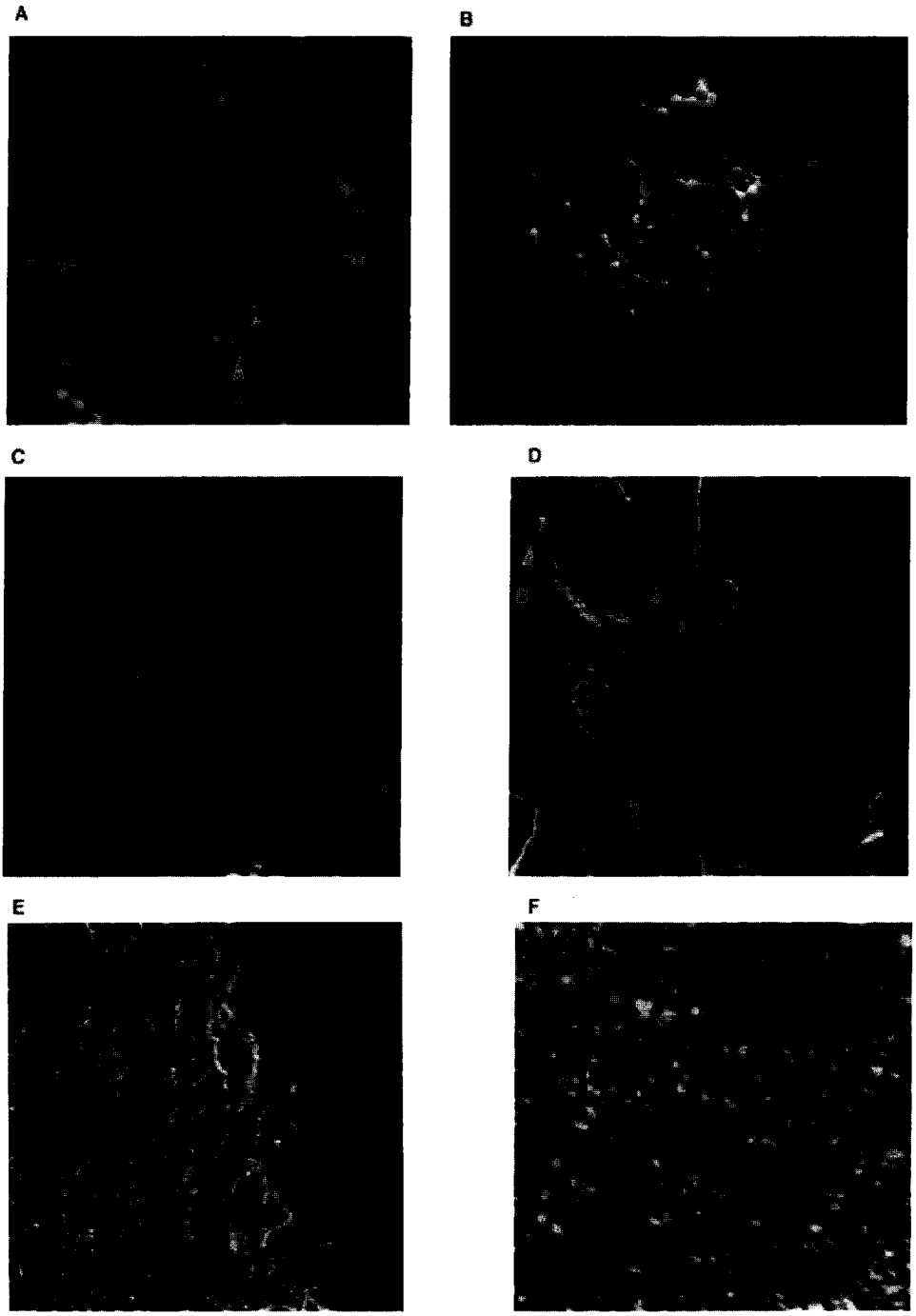

Fig. 1. AFM images of xanthan deposited onto mica: (a) image size 600×600 nm, (b) 3D representation of the image shown in (a), (c) image size 700×700 nm, (d) image size 1000×1000 nm, (e) image size 1500×1500 nm, and (f) image size 1000×1000 nm. Imaging force ca. 3–4 nN. Samples were-air dried onto mica and imaged under butanol.

to find very concentrated regions where the molecules are aligned in bands and bundles (Fig. 1f). These regions contain highly aligned polymer molecules and are similar to the STM images obtained for uncoated xanthan deposited from concentrated liquid crystalline preparations [16]. The major difference appears to be that, in the present case, the molecular alignment is within flat bands rather than the much larger 3D aggregates observed in the STM studies [16].

In the present studies the molecular resolution is limited by probe broadening. From the measured molecular thickness this appears to be of the order of ca. 10 nm. This is comparable to the limitation imposed by grain size in the study of metal-coated samples [17]. However, studies of DNA [28] have shown that the use of supertips can improve resolution. Ideally one would like to obtain information on secondary structure or molecular architecture such as branching. One possible approach is to try to align the molecules side by side. The effects of probe broadening would then be reduced, improving resolution. For this type of study the present sample and imaging methods could be applied. If it were necessary to measure molecular parameters, for example, length distribution or persistence length, a more even coverage of the mica substrate would be appropriate. In order to achieve this it might be useful to combine spray deposition with imaging under butanol.

In conclusion it has been shown that xanthan molecules deposited onto mica can be reliably imaged by AFM. The images obtained in the present study are consistent with images obtained by others using metal-coated samples examined by STM and EM [17]. Our present images differ considerably from the AFM images of continuous periodic arrays reported for xanthan air-dried onto mica [20]. Periodic structures in general should be viewed with caution, unless such defects as polymer ends or dislocations are visible. This is because noise often manifests itself as large arrays of continuous lines with periodic features along their length. The images obtained by Meyer et al. for xanthan deposited from aqueous solution [20] are more reasonable, but appear only to show distorted molecular aggregates with no evidence of single molecules. In this study we have demonstrated, through the use of butanol, the advantages of imaging with very low forces. This allows the fine adjustment of image contrast which is impossible when operating in air, or with the water–mica system, because of the large adhesive forces present (with standard AFM tips). The present images of xanthan are characteristic of polydisperse stiff coils but do show evidence of molecular supercoiling. It remains to be demonstrated whether the present methods can be extended to polysaccharides in general, and whether the resolution can be improved sufficiently to probe secondary structure, molecular architecture such as branching, block structures, or the effects of minor substituents on polymer shape.

Acknowledgements

The authors thank Mike Ridout for preparation of xanthan samples, and Martin Murrell for guidance and advice regarding the use and pitfalls of AFM.

References

[1] R. Guckenberger, T. Hartman, W. Weigrabe, and W. Baumeister, in R. Wiesendanger and H.-J. Guntherodt (Eds.), *Scanning Tunnelling Microscopy II*, Springer Ser. Surf. Sci., Springer-Verlag, Berlin, Heidelberg, 1992, pp 51–98.
[2] A. Engel, *Annu. Rev. Biophys. Chem.*, 20 (1991) 79–108.
[3] V.J. Morris, *Prog. Biophys. Mol. Biol.*, 61 (1994) 131–185.
[4] C.R. Clemmer and T.P. Beebe, *Science*, 251 (1991) 640–642.
[5] W.M. Heckl and G. Binnig, *Ultramicroscopy*, 42–44 (1992) 1073–1078.
[6] G. Travaglini, H. Röhrer, M. Amrein, and H. Gross, *Surf. Sci.*, 181 (1987) 380–390.
[7] M.H. Jericho, B.L. Blackford, and D.C. Dahn, *J. Appl. Phys.*, 65 (1989) 5237–5239.
[8] R. Coratger, A. Chahboun, F. Adjustron, J. Beauvillain, M. Erard, and F. Amalric, *Ultramicroscopy*, 34 (1990) 141–147.
[9] M. Salmeron, T. Beebe, J. Odriozola, T. Wilson, D.F. Ogletree, and W. Siekhaus, *J. Vac. Sci. Technol.*, A8 (1990) 635–641.
[10] M.J. Miles, T.J. McMaster, H.J. Carr, A.S. Tatham, P.R. Shewry, J.M. Field, P.S. Belton, D. Jeenes, B. Hanley, M. Witham, P. Cairns, V.J. Morris, and N. Lambert *J. Vac. Sci. Technol.*, A8 (1990) 698–702.
[11] H. Shigekawa, T. Morozumi, M. Komiyama, M. Yoshimura, A. Kawazu, and Y. Saito, *J. Vac. Sci. Technol.*, B9 (1991) 1189–1192.
[12] Y. Oka and A. Takahashi, *Kobunshi Ronbunshu*, 49 (1992) 389–391.
[13] X. Yang, M.A. Miller, R. Yang, D.F. Evans, and R.D. Edstrom, *FASEB J.*, 4 (1990) 3140–3143.
[14] I. Lee, E.D.T. Atkins, and M.J. Miles, *Ultramicroscopy*, 42–44 (1992) 1107–1112.
[15] M.J. Miles, I. Lee, and E.D.T. Atkins, *J. Vac. Sci. Technol.*, B9 (1991) 1206–1209.
[16] A.P. Gunning, T.J. McMaster, and V.J. Morris, *Carbohydr. Polym.*, 21 (1993) 47–57.
[17] M.J. Wilkins, M.C. Davies, D.E. Jackson, J.R. Mitchell, C.J. Roberts, B.T. Stokke, and S.J.B. Tendler, *Ultramicroscopy*, 48 (1993) 197–201.
[18] J.P. Rabe, S. Bucholz, and A.M. Ritcey, *J. Vac. Sci. Technol.*, A8 (1990) 679–683.
[19] S.L. Tang, A.J. McGhie, and A. Suna, *Phys. Rev.*, B47 (1993) 3850–3856.
[20] A. Meyer, G. Rouquet, K. Lecourtier, and H. Toulhoat, in H. Toulhoat and J. Lecourtier (Eds.), *Physical Chemistry of Colloids and Interfaces in Oil Production*, Editions Technip., Paris, 1992 pp 275–278.
[21] A.L. Weisenhorn, P.K. Hansma, T.R. Albrecht, and C.F. Quate, *Appl. Phys. Lett.*, 54 (1989) 2651–2653.
[22] B. Drake, C.B. Prater, A.L. Weisenhorn, S.A.C. Gould, T.R. Albrecht, C.F. Quate, D.S. Cannell, H.G. Hansma, and P.K. Hansma, *Science*, 243 (1989) 1586–1589.
[23] H.G. Hansma, M. Bezanilla, F. Zenhausern, M. Adrian, and R.L. Sinsheimer, *Nucleic Acids Res.*, 21 (1993) 505–512.
[24] H.G. Hansma, S.A.C. Gould, P.K. Hansma, H.E. Gaub, M.L. Longo, and J.A.N. Zasadzinski, *Langmuir*, 7 (1991) 1051–1054.
[25] H.G. Hansma, J. Vesenka, C. Siegerist, G. Kelderman, H. Morrett, R.L. Sinsheimer, V. Elings, C. Bustamante, and P.K. Hansma, *Science*, 256 (1992) 1180–1184.
[26] H.G. Hansma, R.L. Sinsheimer, M.-Q. Li, and P.K. Hansma, *Nucleic Acids Res.*, 20 (1992) 3585–3590.
[27] M.-Q. Li, H.G. Hansma, J. Vesenka, G. Kelderman, and P.K. Hansma, *J. Biomolec. Sruct. Dyn.*, 10 (1992) 607–617.
[28] M.N. Murray, H.G. Hansma, M. Bezanilla, T. Sano, D.F. Ogletree, W. Kolbe, C.L. Smith, C.R. Cantor, S. Spengler, P.K. Hansma, and M. Salmeron, *Proc. Natl. Acad. Sci. U.S.A.*, 90 (1993) 3811–3814.
[29] T. Coviello, K. Kajiwari, W. Burchard, M. Dentini, and V. Crescenzi, *Macromolecules*, 19 (1986) 2826–2831.
[30] J.P. Cleveland, S. Manne, D. Bocek, and P.K. Hansma, *Rev. Sci. Instrum.*, 64, (1993) 403–405.